Density and distribution of nitrifying guilds in rapid sand filters for drinking water production: Dominance of Nitrospira spp.

Tatari, Karolina; Musovic, Sanin; Gülay, Arda; Dechesne, Arnaud; Albrechtsen, Hans-Jørgen; Smets, Barth F.

Published in:
Water Research

Link to article, DOI:
10.1016/j.watres.2017.10.023

Publication date:
2017

Document Version
Peer reviewed version

Accepted Manuscript

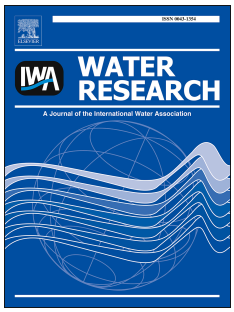

Density and distribution of nitrifying guilds in rapid sand filters for drinking water production: Dominance of *Nitrospira* spp.

Karolina Tatari, Sanin Musovic, Arda Gülay, Arnaud Dechesne, Hans-Jørgen Albrechtsen, Barth F. Smets

PII: S0043-1354(17)30851-5

DOI: 10.1016/j.watres.2017.10.023

Reference: WR 13280

To appear in: *Water Research*

Received Date: 20 March 2017

Revised Date: 7 October 2017

Accepted Date: 9 October 2017

Please cite this article as: Tatari, K., Musovic, S., Gülay, A., Dechesne, A., Albrechtsen, Hans.-Jø., Smets, B.F., Density and distribution of nitrifying guilds in rapid sand filters for drinking water production: Dominance of *Nitrospira* spp., *Water Research* (2017), doi: 10.1016/j.watres.2017.10.023.

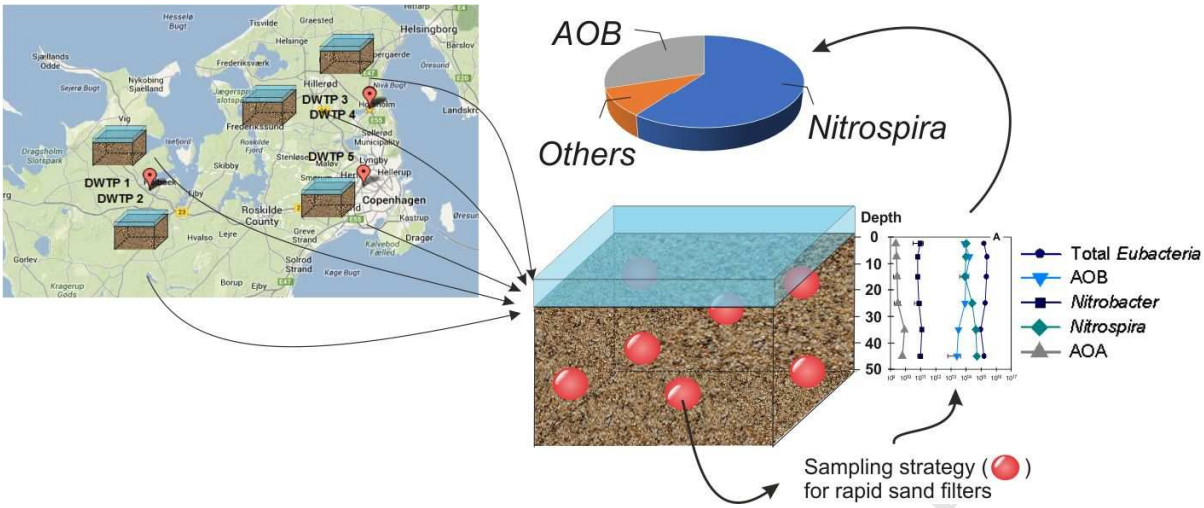

Density and distribution of nitrifying guilds in rapid sand filters for drinking water production: dominance of *Nitrospira* spp.

Karolina Tatari [†], *Sanin Musovic* [†,*], *Arda Gülay, Arnaud Dechesne, Hans-Jørgen Albrechtsen and Barth F. Smets* [‡]

Department of Environmental Engineering, Technical University of Denmark, Miljøvej 113, 2800 Kgs. Lyngby, Denmark

[†]*These authors contributed equally to the manuscript*

**Current Affiliation: Danish Technological Institute, Kongsvang Allé 29, Århus 8000, Denmark*

[‡] *Corresponding author: Tel: +45 45252230, E-mail: bfsm@env.dtu.dk (B. F. Smets)*

Abstract

We investigated the density and distribution of total bacteria, canonical Ammonia Oxidizing Bacteria (AOB) (*Nitrosomonas* plus *Nitrosospira*), Ammonia Oxidizing Archaea (AOA), as well as *Nitrobacter* and *Nitrospira* in rapid sand filters used for groundwater treatment. To investigate the spatial distribution of these guilds, filter material was sampled at four drinking water treatment plants (DWTPs) in parallel filters of the pre- and after-filtration stages at different locations and depths. The target guilds were quantified by qPCR targeting 16S rRNA and *amo*A genes. Total bacterial densities (ignoring 16S rRNA gene copy number variation) were high and ranged from 10^9 to 10^{10} per gram (10^{15} to 10^{16} per m^3) of filter material. All examined guilds, except AOA, were stratified at only one of the four DWTPs. Densities varied spatially within filter (intra-filter variation) at two of the DWTPs and in parallel filters (inter-filter variation) at one of the DWTPs. Variation analysis revealed random sampling as the most efficient strategy to yield accurate mean density estimates, with collection of at least 7 samples suggested to obtain an acceptable (below half order of magnitude) density precision. *Nitrospira* was consistently the most dominant guild (5 to 10% of

total community), and was generally up to 4 orders of magnitude more abundant than *Nitrobacter* and up to 2 orders of magnitude more abundant than canonical AOBs. These results, supplemented with further analysis of the previously reported diversity of *Nitrospira* in the studied DWTPs based on 16S rRNA and *nxrB* gene phylogeny (Gülay et al., 2016; Palomo et al., 2016), indicate that the high *Nitrospira* abundance is due to their comammox (complete ammonia oxidation) physiology. AOA densities were lower than AOB densities, except in the highly stratified filters, where they were of similar abundance. In conclusion, rapid sand filters are microbially dense, with varying degrees of spatial heterogeneity, which requires replicate sampling for a sufficiently precise determination of total microbial community and specific population densities. A consistently high *Nitrospira* to bacterial and archaeal AOB density ratio suggests that non-canonical pathways for nitrification may dominate the examined RSFs.

Keywords

RSF, nitrifying guilds, AOB, NOB, AOA, comammox, Nitrospira

1. Introduction

Rapid sand filters (RSFs) are widely used in groundwater treatment to remove compounds like NH_4^+, Fe^{2+} and Mn^{2+} to below drinking water quality standards; removal occurs by a combination of physico-chemical and biochemical means. The maximum allowed NH_4^+ (and NO_2^-) concentration in the effluent from the drinking water treatment plants (DWTPs) in Europe is 0.5 mg/L (and 0.1 mg/L) (Council Directive 98/93/EC 1998), unless stricter limits are applied by the individual member states (e.g. 0.05 mg/l (and 0.01 mg/L) in DK). NH_4^+ residuals in non-chlorinated systems can cause O_2 consumption in the distribution network (Zhang et al. 2009), as well as accumulation of toxic NO_2^- due to incomplete nitrification (Lytle et al. 2007). In chlorinated distribution systems, NH_4^+ removal is important to control the chlorine residuals and avoid the formation of disinfection byproducts (Lytle et al. 2013, Rittmann et al. 2012).

NH_4^+ removal in RSFs has been assumed to be a two-step biological oxidation process, first to NO_2^- and then to NO_3^-. Oxidation to NO_2^- has typically been attributed to canonical Ammonia Oxidizing Bacteria (AOB) such as *Nitrosomonas* and *Nitrosospira* and Ammonia Oxidizing Archaea (AOA); both AO types have been identified in biological filters (Bai et al. 2013, de Vet et al. 2011, Tatari et al. 2016), although their relative contribution to NH_4^+ removal in these engineered systems has not yet been examined. AOB predominance over AOA seems to link with the NH_4^+ concentration, with lower concentrations favoring the predominance of AOA, potentially due to their higher affinity for NH_4^+ (Martens-Habbena et al., 2009; Niu et al., 2013; Sauder et al., 2012). NO_2^- oxidation in RSFs has been attributed to *Nitrospira* and *Nitrobacter*, although *Nitrospira* has been detected at much higher densities compared to *Nitrobacter* (Albers et al. 2015, Tatari et al. 2016). Additionally, *Nitrospira* but not *Nitrobacter* were detected in a trickling filter treating groundwater (de Vet et al. 2009).

Few studies have reported on densities of different nitrifying guilds, yet such information might provide clues on the importance of different guilds in the overall RSF performance (i.e. ammonia removal) under certain operational conditions. In trickling filters treating groundwater, mean filter densities of AOB (10^7-10^9 AOB cells /g filter material) vastly exceeded those of AOA (10^5 cells /g filter material) as quantified by *amo*A-based qPCR (de Vet et al. 2009). AOB mean densities of 10^6-10^9 copies/g filter material were reported (quantified by *amo*A-based qPCR) for granular activated carbon filters treating surface water (Niu et al. 2013). The large range in reported densities (for single systems) would seem worrying, yet quantification of total bacteria, AOB and AOA in biological sand filters has occasionally revealed substantial depth stratification and spatial variation (Bai et al. 2013, Lee et al. 2014, Tatari et al. 2016, Gülay et al., 2016). Hence, appropriate sampling may be essential to ensure representative density estimates of microbial guilds in RSFs.

Relative densities of different microbial guilds can also be compared to predicted ratios based on assumed physiology and stoichiometry; large deviations would then challenge the underlying assumptions. Recently we discovered anomalous relative densities *Nitrospira* to AOB in RSFs, with *Nitrospira* comprising up to 45% of all community 16S rRNA gene amplicons with canonical AOB attaining on average 2.5% (Gülay et

al., 2016). These unexpectedly high *Nitrospira* densities do not agree with stoichiometry assuming *Nitrospira* to have physiology of a nitrite oxidizing bacterium (NOB), which would predict ratios of AOB to NOB of 2 to 3 (Hagopian and Riley 1998, Winkler et al. 2012). Recently, some *Nitrospira* types have been found to carry a full set of *amo* and *hao* genes, which may enable them to oxidize also NH_4^+ and therefore carry out complete NH_4^+ (to NO_3^-) oxidation; all *amo* containing *Nitrospira* described to date belong to *Nitrospira* sublineage II (Daims et al. 2015, Palomo et al. 2016, van Kessel et al. 2015, Pinto et al., 2015). Nevertheless, direct proof for NH_4^+ oxidizing activity by *Nitrospira* in RSFs has not yet been provided.

This work addressed the following questions. First, is there significant spatial variation in the distribution of total bacteria and nitrifying guilds (AOB, AOA, *Nitrobacter* and *Nitrospira*) in RSFs? Second, do the relative densities of the nitrifying guilds agree with their expected roles and physiologies in RSFs? Hence, we conducted an extensive and spatially explicit survey of nitrifying guilds in replicate filters at 4 DWTPs. The data were used to examine spatial variation, and identify optimal sampling strategies. Relative density ratios were examined and related to the operating conditions to infer roles of the different guild members. Finally, given the consistently high *Nitrospira* presence, we assessed the relative abundance of *Nitrospira* sublineages based on *nxrB* and 16S rRNA gene analysis.

2. Materials & Methods

2.1. Overview of the investigated DWTPs

The investigations included four Danish DWTPs treating groundwater that have been in operation for 6 to 40 years. Groundwater at the investigated DWTPs is abstracted from deep limestone anoxic aquifers and the treatment train consists of an aeration step and a double filtration step. Pre-filters have a bed of coarse sand material and are intended to retain the Fe-hydroxides, formed by the oxidation of Fe^{2+}. Pre-filter effluent is supplied to the after-filters, which consists of a 0.4 to 0.7 m deep bed of fine sand on top of gravel. Design parameters and selected water quality characteristics at the investigated DWTPs are summarized in Table 1. Pre- and after-filters at the investigated DWTPs are backwashed at regular times by air scouring followed by high water flowrates (Table 1).

DWTP 1 and 2 are located at Sjælsø (Nordvand A/S), in the greater Copenhagen area. The two DWTPs are operated independently and receive raw water with significantly different CH_4 content (Table 1). DWTP 3 (Langerød) is located in Holbæk (Fors A/S) and consists of two parallel lines, West and East (W, E) which were operated nearly identically, but displayed different performance with regards to NH_4^+ removal (effluent NH_4^+ concentration 0.05 and 0.15 mg/L from E and W, respectively). DWTP 4 is Islevbro waterworks (HOFOR A/S) located in the greater Copenhagen area, and has very low NH_4^+ and CH_4 concentrations in the raw water (Table 1).

2.2. Filter material sampling

Microbial density was quantified for filter material collected from the pre- and after-filters at the investigated DWTPs. The sampling strategy was designed to investigate depth stratification, spatial variation within a filter (intra-filter variation) and variation between parallel filters (inter-filter variation). Filter material was core-sampled using a Plexiglas cylinder (1 m height and 5 cm inner diameter), closed on the one end with a rubber stopper. The sampler was pushed into the filter and gently pulled retaining a 40-60 cm filter material core. One pre-filter was sampled at 1-3 random locations at DWTPs 1-3. The pre-filters at DWTP 4 could not be sampled because of the coarse filter material (Table 1) that could not be collected with the core sampler. 2-3 parallel after-filters were sampled at all DWTPs, and a filter material core was collected from 1-3 randomly selected locations in each filter. All cores were sampled at approximately 2/3 of a filter run cycle between two consecutive backwashing events. The filter material cores were divided into the following depth segments: 0-5, 5-10, 10-20, 20-30, 30-40, 40-50 cm that were transferred to the lab on ice and frozen until further analysis.

2.3. Quantification of the selected microbial guilds by qPCR

The density of total bacteria (*Eubacteria*), β-proteobacterial AOB (*Nitrosomonas* spp and *Nitrosospira* spp), *Nitrobacter* spp, and *Nitrospira* spp was quantified by 16S rRNA gene targeted qPCR in each filter material segment. DNA was extracted from 0.5 g drained filter material using MP FastDNA SPIN Kit (MP Biomedicals LLC) previously shown effective for DNA extraction from iron oxide rich environments (Kato et al. 2013). Earlier efforts at removing/solubilizing metal oxides by pretreatment with oxalic acid did not

115 enhance DNA recovery, and neither did pretreatment by sonication. The extracted DNA was eluted in 100 µl
116 Tris-EDTA buffer and its concentration and purity estimated by measuring absorbance at 260 and 280 nm
117 (NanoDrop). A group specific region on the 16S ribosomal-RNA encoding the rrs gene (16S rRNA) was
118 targeted by the primer sets 1055f and 1392R for total bacteria (Ferris et al. 1996, Lane 1991), CTO189A/B/C
119 and RT1 for β-proteobacterial AOB genera *Nitrosomonas* and *Nitrosospira* (Hermansson and Lindgren
120 2001), Nspra675f and Nspra746r for the *Nitrospira* genus (Graham et al. 2007) and FGPS872f and
121 FGPS1269r for the *Nitrobacter* genus (Degrange and Bardin 1995). AOB and AOA were also quantified by
122 *amo*A targeted qPCR, using the amoA1f and amoA2r primers for β-proteobacterial AOB (Rotthauwe et al.
123 1997) and the amoAF and amoAR primers for AOA (Francis et al. 2005). Specificity of the 16S rRNA and
124 *amoA* targeted primers for beta-proteobacterial AOB was confirmed and published separately (Dechesne et
125 al., 2016); specificity of the *amoA* targeted primers for AOA was confirmed here by clone library analysis;
126 the 16S rRNA targeted primers for *Nitrospira* were confirmed *post hoc* by *in silico* comparison with the 16S
127 rRNA amplicon libraries of the same samples (Gülay et al. 2016) to be specific and cover 96% cover of all
128 *Nitrospira* diversity.

129 The qPCR analyses were run in duplicate in a Chromo4 thermocycler using the Opticon Monitor 3 software
130 (Bio-Rad Laboratories). Each qPCR reaction contained 12.5 µl of 2×iQ SYBR Green Supermix (Bio-Rad
131 Laboratories), 500 nM of each primer, DNA template (10 ng) and DNA/RNA-free water (Mol. Bio.) to 25
132 µl. The thermal cycling conditions consisted of an initial 5 min denaturation at 95°C, followed by 40 cycles
133 of 30 s at 94°C, primer annealing for 30 s at 55°C for total bacteria, 30 s at 60/56°C for AOB (16S-rRNA),
134 60 s at 50°C for *Nitrobacter*, 30 s at 64°C for *Nitrospira*, 60 s at 60°C for AOA (*amo*A), 40 s at 55°C for
135 AOB (*amo*A), and 1 min extension at 72°C. After the 40th cycle, a final DNA extension at 72°C for 10 min
136 was performed followed by cooling at 4°C. The melting curve analysis (gradient 0.2°C/s, range 70-95°C)
137 (Ririe et al. 1997) showed single peaks for all qPCR reactions. Reported qPCR reactions had amplification
138 efficiencies between 97 and 100%; addition of BSA (to address potential PCR inhibition) had no further
139 positive effect. The gene copy number was obtained by comparing the cycle threshold values of the sample

against a standard curve for each qPCR target. To express microbial densities per unit volume of filter material, bulk densities at each depth were calculated by weighing 10-20 mL of drained filter material.

2.4. Statistical analysis of microbial densities

The measured densities in pre- and after-filters were statistically analyzed to assess their spatial variation at three levels: depth stratification, intra-filter variation and inter-filter variation. Spearman's rank correlation tests (α=0.05) were performed to examine the correlation between density of a specific guild and filter depth. To investigate intra-filter variation, the depth profiles from distinct locations in a filter were tested for differences by paired t-tests (α=0.05) in all possible combinations. Lastly, inter-filter variation was investigated by paired t-tests (α=0.05) on mean depth profiles in parallel filters. The mean depth profile in a filter was calculated as the mean density at each depth for all sampling locations.

To assess how the sampling effort relates to the measured average density of a specific guild, we examined the distribution of the total bacterial mean density in the after-filters. This analysis examined three sampling strategies: random sampling, sampling at different depths and sampling at different locations. Detailed information about statistical analyses is provided in the Supplemental Information (SI).

2.5. Bioinformatic analysis

We evaluated the lineages that constitute the comammox *Nitrospira* population genome CG24 earlier identified in DWTP 4 (Palomo et al., 2016) and the *Nitrospira* distribution across its lineages at all DWTPs based on earlier published 16S rRNA amplicon libraries (Gülay et al., 2016). Details on bioinformatics analysis are in the SI.

3. Results & Discussion

3.1. Density of total bacteria, AOB, *Nitrobacter*, *Nitrospira* and AOA in RSFs

The targeted microbial guilds were quantified by qPCR in the filter material collected from the pre- and after-filters. Filter material density and microbial density values are reported (Table 2) as means of the

densities at all depths, all sampled locations and all parallel filters for each filtration stage at each DWTP. The mean filter material densities were in the range of 1.0-1.7×10^6 g/m^3 (Table 2), with variation caused by the different filter material types and sizes (Table 1) and degrees of mineral coating (Gülay et al. 2014).

Microbial densities, measured per unit filter material mass, are readily converted into volume using the estimated filter material densities. While both density expressions are presented (Table 2) for the examined guilds, the following discussion considers volumetric densities.

Total bacterial (*Eubacteria*) 16S rRNA gene densities ranged from 1.1 to 16×10^{15} copies/m^3 filter material (Table 2). The density was highest in the pre-filters at DWTP 2, and was substantially higher than the density in the after-filters at the same DWTP (Table 2). At the other investigated DWTPs, bacterial density was similar in pre- and after-filters (Table 2). The high density observed in the pre-filters is surprising, as pre-filters were historically thought to remove primarily Fe^{2+} and mainly through chemical oxidation and precipitation (Sharma et al., 2005). It appears that the resulting oxy-hydroxide precipitates provide a highly-porous mineral coating on the filter grains, which can support the high microbial density (Gülay et al., 2014).

Canonical AOB (*Nitrosomonas* spp. and *Nitrosospira* spp.) were identified in all investigated filters at 16S rRNA gene densities ranging from 0.5 to 35×10^{13} copies/m^3 filter material. Densities in the pre-filters were higher than in the after-filters at all DWTPs, with one exception (DWTP 3-E, Table 2). High AOB densities in the pre-filters indicate that NH_4^+ removal takes place in both filtration steps. For example, at DWTP 3 the NH_4^+ concentrations after aeration were 0.89-0.94 mg/L and decreased to 0.54-0.75 after the prefilters and further to 0.007-0.1 mg/L after the after filters. This waterworks (DWTP 3) had different nitrification behaviors in the parallel lines: DWTP 3-W consistently removed NH_4^+-N more efficiently and to a lower level (e.g. 0.007-0.01 mg/L) than DWPT3-E (e.g. 0.077-0.11 mg/L), which is reflected by a higher AOB density (particularly in the prefilters) in DWTP 3-W than in DWTP 3-E (Table 2).

Nitrobacter 16S rRNA gene densities ranged across two orders of magnitude: from 3.6 to 500×10^{10} copies/m^3 in the investigated filters (Table 2). *Nitrobacter* pre-filter densities were higher than the respective after-filter densities at all DWTPs. *Nitrospira* were present in all investigated filters at 16S rRNA gene

189 densities ranging from 0.97 to 33×10^{14} copies/m^3 filter material. *Nitrospira* densities at two waterworks
190 (DWTPs 1 and 2) were slightly (4 to 6 fold) higher in pre-filter versus after-filters, with the opposite trend in
191 a third waterworks (DWTP 3, Table 2). Consistently, *Nitrospira* densities were at least 2 orders of magnitude
192 higher than *Nitrobacter* densities, suggesting *Nitrospira* as dominant NO_2^- oxidizer at all DWTPs. Another
193 study on Danish DWTPs reports that *Nitrospira* accounted for up to 8% of all prokaryotic amplicon
194 sequences and detected no *Nitrobacter* sequences in RSFs (Albers et al. 2015); however the lack of
195 replication and the exceedingly small amplicon library size (558 sequences/samples) challenge the
196 robustness of those observations. Similarly *Nitrospira*, but not *Nitrobacter*, were detected by DGGE analysis
197 of 16S rRNA gene fragments from a groundwater fed trickling filter (de Vet et al. 2009). *Nitrospira*
198 sequences also accounted for up to 51% of the clone library in samples from an anthracite/sand dual media
199 filter fed with groundwater (White et al. 2012). Finally, in our microbial community diversity analysis on the
200 same DWTPs, we similarly observed *Nitrospira* sp. as the most abundant taxon in the 16S rRNA amplicon
201 libraries (from 19% to 71% in all DWTPs (Gülay et al., 2016)).

202 AOA *amoA* gene densities were below detection limits in one of the after-filters (DWTP 3), while at the
203 other waterworks their densities ranged from 4.0 and 20×10^9 copies/m^3 filter material. AOA were typically 4
204 orders of magnitude less abundant than AOBs, except in the DWTP 4 after-filters, where highest AOA
205 densities were observed (Table 2).

206 Overall, RSF are microbially dense, and the targeted guilds are often at least as heavily present in the pre-
207 filters as in the after-filters, revealing an important role of pre-filters in biological processes.

208 3.2. Spatial distribution of the investigated microbial guilds

209 In the pre-filters, limited stratification was observed (except in DWTP 2, where AOB and *Nitrospira*
210 densities decreased with depth and in DWTP 1 where *Nitrospira* densities increased with depth (Fig 1, Table
211 SI 1)). Stratification in the after-filters was noted for some microbial guilds at DWTP 2 and 3, and for all
212 microbial guilds (except AOA) at DWTP 4 (Fig. 1, Table SI 2), with densities decreasing with depth. No
213 stratification was observed in the after-filters at DWTP 1 (Fig. 1).

Backwashing frequency and strategy are crucial to control the mixing and redistribution of the filter material, eventually preventing or allowing permanent stratification in the filter. Stratification at DWTP 3 and 4 is maintained after backwashing due to the presence of substantial mineral coatings on the filter material grains, which forces larger – and less dense grains – to remain at the top of the filter, and smaller – denser grains – to settle in deeper filter regions, thus maintaining a permanent distribution (Gülay et al. 2014). In line with these observations, sand grains in DWTP 1 and 2 have a very low degree of mineral coating at all depth levels and show no evidence of biomass stratification (Gülay et al. 2014). Depth stratification in groundwater-fed periodically backwashed RSFs has been observed before (Bai et al. 2013).

In individual pre-filters, replicate profiles at different sampling locations yielded essentially similar density distributions for all microbial populations (except for *Nitrobacter* (Table SI 3)) and the same was observed in the after-filters (Table SI 4). This stands in contrast to previous studies (at DWTP 1) which documented local hydraulic heterogeneity in both pre- and after-filters, and suggested a strong effect on local NH_4^+ removal rate (Lopato et al. 2011, Lopato et al. 2013). Clearly, the hydraulic heterogeneity does not result in observable differences in horizontal densities of microbial groups.

However, parallel after-filters at a DWTP often had different profiles: densities of total bacteria, AOB and *Nitrospira* varied across the filters of both lines at DWTP 3, whereas 50% of the compared profiles were significantly different at DWTP 4 and no significant variation was observed at DWTP 1 and 2 (Tables SI 5-7). Inter-filter variation at both lines of DWTP 3 was much larger than the intra-filter variation, and the opposite was observed at DWTPs 1 and 2. Hence, spatial variation of the targeted guilds does not follow a predictable pattern at the investigated DWTPs.

3.3. Investigation of mean density precision and required sampling effort

The increase in precision of the estimated mean density was evaluated as a function of sampling effort and sampling strategy ((i) random sampling of *s* samples across locations, parallel filters, and depth; (ii) sampling all locations for *d* randomly chosen depths; (iii) and sampling full profiles at *l* randomly chosen locations). Setting half-an-order of magnitude as an acceptable precision, the mean density and associated precision

were computed at the investigated DWTPs: clearly precision increased with increasing sampling effort (Fig. 2, Fig. SI 1). With DWTP 4 as an example, sampling at 7 random combinations of locations and depths was required to meet the demanded precision (Fig. 2). Sampling at different depths would require 14 samples (2 randomly chosen depths at all investigated filter locations and parallel filters), sampling at different locations and filters would require 17 samples (at least 3 locations, each location sampled at 5-6 depths). Clearly random sampling yielded an acceptably precise density estimate with lowest effort, and there was no advantage of exhaustively sampling depths profiles or horizontal profiles.

The mean bacterial density estimates were more precise at DWTPs 1-3, where collection of a singular sample would already give an estimate within half-an-order of magnitude precision (Fig. SI 1). For almost all DWTPs, random sampling yields the highest precision compared to sampling at different depths or locations (Fig. SI 1). The only exception was at DWTP 3-W, where sampling of 1 filter location at all depths (7 samples) yields a higher precision than collecting 7 random samples (Fig. SI 1). However, fewer than 7 samples are required to obtain a mean precision above the acceptable limit of half-an-order of magnitude.

Overall, the mean density precision can vary significantly at different DWTPs. In all cases random sampling across filters, filter locations and depths yielded the highest precision for a given number of samples. According to the precision required by each study, the number of samples needed may vary significantly. In this study, each sample had a mass of 100-333 g drained filter material, depending on the depth interval (segmented every 5 or 10 cm as described in sec. 2.2) and the bulk density. Ultimately, 7 samples randomly collected should generally be sufficient to provide a precision of the mean of half order of magnitude, even at DWTPs with heterogeneous microbial spatial distributions. Our recommendations apply to density, but may not apply to community diversity or composition. When the same samples were subject to community analysis via 16S rRNA amplicon sequencing, triplicate samples within a RSF were compositionally different from each other at the whole community level (Gülay et al., 2016); yet were identical in terms of dominant taxa (>1%) (Gülay and Smets, 2015).

3.4. Relative abundance of microbial guilds

The fraction of canonical AOB (abundance vs total bacteria) ranged from 0.004 and 0.07 in the pre-filters, and from 0.002 and 0.12 in the after-filters (Fig. 3, Panels A and D). Abundances in the pre- and after-filters were similar at most DWTPs except at DWTP 1, where abundance in the pre-filters was approximately one order of magnitude higher than in the after-filters. No patterns were observed with depth.

The ratio of canonical AOB to *Nitrospira* ranged from 0.02 and 1.9 in the pre-filters, and from 0.04 and 0.6 in the after-filters (Fig. 3, Panels B and D). Ratios were consistently below 1 in all RSFs except in one set of pre-filters (DWTP 1), where AOB were more dominant than *Nitrospira* in the filter top (ratio 1.9). Even here, an increase in *Nitrospira* density with depth (Table SI 1) made AOB less dominant than *Nitrospira* at the bottom of the filter (ratio 0.05). Overall, while the proportions varied, canonical AOB (i.e. Nitrosomonas plus Nitrosospira *genus*) were consistently less abundant than *Nitrospira* genus.

Similar anomalous *Nitrospira* to *Nitrosomonas* (or more correctly *Nitrosomonas* + *Nitrosospira*) abundance ratios have been reported by others. These reports were based on relative sequence abundances in clone or amplicon libraries in both groundwater (e.g. 3.7% vs 33.4% (Nitzsche et al. 2015); 3.2% vs 16.9% (White et al. 2012) *Nitrosomonas* and *Nitrospira* abundance, respectively) and surface water fed drinking water treatment gravity filters (0.8% vs 17.3% (Feng et al. 2012), 0.07% vs 17 *Nitrosomonas* and *Nitrospira* abundance, respectively (LaPara et al. 2015)). Proposed, yet unproven, explanations for these observations were PCR primer bias, differences in 16S rRNA gene copy numbers (Nitzsche et al. 2015), presence of unidentified NH_4^+ oxidizers (LaPara et al. 2015) and presence of dormant *Nitrospira* cells (Martiny et al. 2005). Winkler et al. (2012) proposed that unexpectedly high NO_2^- oxidizer (e.g. *Nitrospira*) abundance in a community may also be caused by a NO_2^- oxidation/NO_3^- reduction loop, which would be driven by incomplete heterotrophic denitrification. While bulk phase dissolved oxygen concentrations in both pre- and after-filters are near saturation, strictly heterotrophic anaerobes (*Xanthomonadales* and *Anaerolineales*) have been reported in amplicon libraries of the after-filters (Gülay et al., 2016), and existence of the proposed NO_2^-/ NO_3^- loop, and its contribution to the observed *Nitrospira* abundance should be examined.

Recent discoveries have revealed that the physiological abilities of *Nitrospira* may extend far beyond NO_2^- oxidation. Genomic and physiological evidence has shown that certain *Nitrospira* strains can oxidize hydrogen, cyanate and simple organic compounds such as formate (Koch et al., 2014) (Palatinszky et al., 2015) . The chemical nature of the groundwater and the initial aeration/stripping makes cyanate or hydrogen unlikely candidates to support *Nitrospira* growth, especially in the downflow units. Similarly, because assimilable organic carbon in the feed groundwater is low, only decay products from the RSF microbiome would be available to support heterotrophic *Nitrospira* growth. The qPCR results, and our previous 454 survey (Gülay et al., 2016), indicate that *Nitrospira* is the most abundant taxon: such abundance is not likely supported by metabolic decay products of a microbial community. Of specific interest is the recent discovery that some *Nitrospira* genomes harbor *amo* genes and have the potential for NH_4^+ oxidation – in addition to NO_2^- oxidation – endowing them the physiology of complete ammonia oxidation (comammox) (Daims et al., 2015; Palomo et al., 2016; Pinto et al., 2015; van Kessel et al., 2015). The described enriched and isolated comammox *Nitrospira* strains - *Candidatus Nitrospira inopinata*, *Cand N. nitrosa* and *Cand. N. nitrificans* (Daims et al., 2015)(van Kessel et al., 2015) – all belong to *Nitrospira* lineage II, with *N. moscoviensis* as best known canonical NOB as reference strain (Pester et al., 2014).

Given the striking dominance of the *Nitrospira* genus in all DWTPs (Fig. 1, Table 2), we analyzed its composition across *Nitrospira* lineages from the 16S rRNA amplicon libraries at the same DWTPs (Gülay et al., 2016): *Nitrospira* lineage II dominated at all DWTPs, representing consistently over 95%, with not-yet-named lineages accounting for 3.5%±0.03, of all *Nitrospira* reads (Fig. 4 Fig SI 2, Table SI 8).

Earlier, we identified, from the DWTP 4 metagenome, a *Nitrospira* population genome with comammox capability (CG_24) (Palomo et al., 2016). This population genome consisted of several sub-genomes, but no efforts were made to separate the individual genomes and examine their phylogeny. Here – based on phylogenetic analysis of CG24's *nxrB* content - we show that the five different constituent *nxrB* sequence types are lineage II (Fig. 4). As *nxrB* and 16S rRNA genes yield congruent *Nitrospira* phylogenies (Pester et al., 2014), and given the high abundance of CG24 in the community metagenome (up to 30 % of all mapped reads (Palomo et al., 2016)); *Nitrospira* in DWTP 4 are likely primarily comammox *Nitrospira*. By

extension, these results indicates that the high *Nitrospira* abundances (compared to canonical AOBs) in all examined DWTPs are, to a large extent, the result of the NH_4^+ oxidation capability of *Nitrospira.*

AOA were consistently less abundant than AOB (based on *amo*A targeted qPCR) in both pre- and after-filters at DWTPs 1, 2, and 3, (Fig. 3, Panels C and F) and occasionally at or below detection limit. AOA have been identified in other drinking water treatment plants – where occasionally they are abundant (Kasuga et al., 2010; van der Wielen et al., 2009). When detected in this study, the AOA/AOB ratios ranged between 3×10^{-6} and 8×10^{-3} in the pre-filters, and between 2×10^{-5} and 0.2 in the after-filters. While the AOA/AOB ratios were calculated based on archaeal and bacterial *amo*A targeted qPCR, quantification based on the chosen *amoA* PCR primers (Rotthauwe et al. 1997) underestimates AOB densities (based on 16S rRNA targeted qPCR) at some DWTPs (DWTPs 1, 2 and 4 but not at DWTP 3 (Fig. SI 3)). This underestimation was recently identified as caused by the preferential amplification of *amoA* Cluster 7 vs. Cluster 6A AOBs (Dechesne et al. 2016). In addition, the employed *amoA* primers would not quantify comammox *amoA* (Daims et al. 2015). Considering this bias, the AOA to AOB ratios at DWTPs 1 and 2 would be even lower. No consistent trend of the AOA/AOB ratio with depth was observed at any of these DWTPs. AOAs were at significant abundance compared to AOB in only one of the waterworks (DWTP 4) (AOA/AOB from 0.26 in the top 0-5 cm to 20 at the bottom 40-50 cm (Fig. 3, Panel F)). The increased ratio (by roughly 2 orders of magnitude) was mainly due a reduction in AOB abundance (Fig. 1, Panel C) and may suggest a significant role of AOA at the bottom of the filter. Yet, as *amo*A based qPCR also underestimates AOB densities at DWTP 4 (Fig SI 3), the true ratios are higher and AOA may have a secondary role even at the bottom of the filter at DWTP 4. The relative enrichment of AOA over AOB at the filter base (with lower NH_4^+ supply) is, nevertheless, consistent with the notion that AOA are competitive over AOB in conditions of reduced energy supply, such as in soils (Leininger et al. 2006, Verhamme et al. 2011) and ocean (Wuchter et al. 2006), most likely due to their ability to cope with energy stress (Martens-Habbena et al. 2009, Valentine 2007). At the system level, similar correlations between AOA and AOB predominance and NH_4^+ loading are apparent, with AOB densities (in both pre- and after-filters) increasing with loadings, and AOA densities decreasing

with loading (Fig. 5) consistent with observations that AOA densities increase inversely with ammonium gradients (Sauder et al., 2012).

In sum, notwithstanding the relatively low influent ammonium concentrations (max. 1 mg/L) at all DWTPs canonical AOB are numerically dominant over AOA, and both are vastly inferior to *Nitrospira*.

4. Conclusions

This work presents the first comprehensive investigation of the density and spatial distribution of total bacteria, AOB, *Nitrobacter*, *Nitrospira* and AOA by qPCR at a number of full scale DWTPs. The main conclusions are:

- Microbial density can vary spatially in a filter and in parallel filters at a DWTP. Specifically, we observed strong stratification of nitrifying guilds in one DWTP, but not in others. Horizontally, intra- or/and inter filter variation were significant at the investigated DWTPs, indicating the need of proper experimental design to obtain representative results.
- Variation analysis for total bacteria estimated that 7 random filter material samples need to be collected at a DWTP with high spatial variation to obtain an acceptable precision for the mean (half an order of magnitude). At the other investigated DWTPs, one sample collected from a random location can already provide a density estimate within an acceptable (half an order of magnitude) precision interval. Higher sample replication will typically be required if the goal is to describe mean microbial community composition (Gulay et al, 2016)
- *Nitrospira* were roughly 4 orders of magnitude more abundant than *Nitrobacter* in all investigated filters, suggesting that they should be the predominant NO_2^- oxidizers. Yet, *Nitrospira* were also up to almost 2 orders of magnitude more abundant than AOBs, and we suggest that the Nitrospira abundance is primarily caused by their NH_4^+ oxidation capability (comammox).

- Among the canonical ammonia oxidizers, AOB exceed AOAs in RSFs, except in RSFs with strong stratification; and AOB are favored at DWTPs operating at higher loading rates.

Acknowledgments

We thank Florian Wagner for assistance in preparing Table 1 and providing valuable feedback on the manuscript. This work was supported by the Danish Council for Strategic Research (Grant agreement number: KBBE- 2012-6-311846) via the project DW-Biofilters.

References

Albers, C.N., Ellegaard-Jensen, L., Harder, C.B., Rosendahl, S., Knudsen, B.E., Ekelund, F. and Aamand, J. (2015) Groundwater chemistry determines the prokaryotic community structure of waterworks sand filters. Environmental Science & Technology 49(2), 839-846.

Bai, Y., Liu, R., Liang, J. and Qu, J. (2013) Integrated metagenomic and physiochemical analyses to evaluate the potential role of microbes in the sand filter of a drinking water treatment system. Plos One 8(4).

Council Directive 98/93/EC (1998) Quality of Water Intended for Human Consumption, Annex I, Part C.

Daims, H., Lebedeva, E.V., Pjevac, P., Han, P., Herbold, C., Albertsen, M., Jehmlich, N., Palatinszky, M., Vierheilig, J., Bulaev, A., Kirkegaard, R.H., von Bergen, M., Rattei, T., Bendinger, B., Nielsen, P.H. and Wagner, M. (2015) Complete nitrification by Nitrospira bacteria. Nature 528(7583), 504-+.

de Vet, W., Dinkla, I.J.T., Muyzer, G., Rietveld, L.C. and van Loosdrecht, M.C.M. (2009) Molecular characterization of microbial populations in groundwater sources and sand filters for drinking water production. Water Research 43(1), 182-194.

de Vet, W., Kleerebezem, R., van der Wielen, P., Rietveld, L.C. and van Loosdrecht, M.C.M. (2011) Assessment of nitrification in groundwater filters for drinking water production by qPCR and activity measurement. Water Research 45(13), 4008-4018.

Dechesne, A., Musovic, S., Palomo, A., Diwan, V. and Smets, B.F. (2016) Underestimation of ammonia-oxidizing bacteria abundance by amplification bias in amoA-targeted qPCR. Microbial Biotechnology 9(4), 519-524.

Degrange, V. and Bardin, R. (1995) Detection and counting of Nitrobacter populations in soil by Pcr. Applied and Environmental Microbiology 61(6), 2093-2098.

Feng, S., Xie, S., Zhang, X., Yang, Z., Ding, W., Liao, X., Liu, Y. and Chen, C. (2012) Ammonium removal pathways and microbial community in GAC-sand dual media filter in drinking water treatment. Journal of Environmental Sciences 24(9), 1587-1593.

Ferris, M.J., Muyzer, G. and Ward, D.M. (1996) Denaturing gradient gel electrophoresis profiles of 16S rRNA-defined populations inhabiting a hot spring microbial mat community. Applied and Environmental Microbiology 62(2), 340-346.

Francis, C.A., Roberts, K.J., Beman, J.M., Santoro, A.E. and Oakley, B.B. (2005) Ubiquity and diversity of ammonia-oxidizing archaea in water columns and sediments of the ocean. Proceedings of the National Academy of Sciences of the United States of America 102(41), 14683-14688.

Frey, S.D., Elliott, E.T. and Paustian, K. (1999) Bacterial and fungal abundance and biomass in conventional and no-tillage agroecosystems along two climatic gradients. Soil Biology & Biochemistry 31(4), 573-585.

Graham, D.W., Knapp, C.W., Van Vleck, E.S., Bloor, K., Lane, T.B. and Graham, C.E. (2007) Experimental demonstration of chaotic instability in biological nitrification. Isme Journal 1(5), 385-393.

Gülay, A., Musovic, S., Albrechtsen, H.-J., Al-Soud, W.A., Sørensen, S.J., Smets, B.F., 2016. Ecological patterns, diversity and core taxa of microbial communities in groundwater-fed rapid gravity filters. ISME J.

10, 2209–2222.

Gülay, A., Tatari, K., Musovic, S., Mateiu, R.V., Albrechtsen, H.-J. and Smets, B.F. (2014) Internal porosity of mineral coating supports microbial activity in rapid sand filters for groundwater treatment. Applied and Environmental Microbiology 80(22), 7010-7020.

Hagopian, D.S. and Riley, J.G. (1998) A closer look at the bacteriology of nitrification. Aquacultural Engineering 18(4), 223-244.

Hermansson, A. and Lindgren, P.E. (2001) Quantification of ammonia-oxidizing bacteria in arable soil by real-time PCR. Applied and Environmental Microbiology 67(2), 972-976.

Kasuga, I., Nakagaki, H., Kurisu, F., Furumai, H., 2010. Predominance of ammonia-oxidizing archaea on granular activated carbon used in a full-scale advanced drinking water treatment plant. Water Res. 44, 5039–49.

Kato, S., Chan, C., Itoh, T., Ohkuma, M., 2013. Functional Gene Analysis of Freshwater Iron-Rich Flocs at Circumneutral pH and Isolation of a Stalk-Forming Microaerophilic Iron-Oxidizing Bacterium. Appl. Environ. Microbiol. 79, 5283–5290.

Koch, H., Galushko, A., Albertsen, M., Schintlmeister, A., Gruber-Dorninger, C., Lucker, S., Pelletier, E., Le Paslier, D., Spieck, E., Richter, A., Nielsen, P.H., Wagner, M., Daims, H., 2014. Growth of nitrite-oxidizing bacteria by aerobic hydrogen oxidation. Science (80-.). 345, 1052–1054.

Lane, D.J. (1991) Nucleic acid techniques in bacterial systematics, pp. 115-175, John Wiley and Sons, New York.

LaPara, T.M., Wilkinson, K.H., Strait, J.M., Hozalski, R.M., Sadowksy, M.J. and Hamilton, M.J. (2015) The Bacterial Communities of Full-Scale Biologically Active, Granular Activated Carbon Filters Are Stable and Diverse and Potentially Contain Novel Ammonia-Oxidizing Microorganisms. Applied and Environmental Microbiology 81(19), 6864-6872.

Lee, C.O., Boe-Hansen, R., Musovic, S., Smets, B., Albrechtsen, H.J. and Binning, P. (2014) Effects of dynamic operating conditions on nitrification in biological rapid sand filters for drinking water treatment. Water Research 64, 226-236.

Leininger, S., Urich, T., Schloter, M., Schwark, L., Qi, J., Nicol, G.W., Prosser, J.I., Schuster, S.C. and Schleper, C. (2006) Archaea predominate among ammonia-oxidizing prokaryotes in soils. Nature 442(7104), 806-809.

Lopato, L., Galaj, Z., Delpont, S., Binning, P.J. and Arvin, E. (2011) Heterogeneity of Rapid Sand Filters and Its Effect on Contaminant Transport and Nitrification Performance. Journal of Environmental Engineering-Asce 137(4), 248-257.

Lopato, L., Rottgers, N., Binning, P.J. and Arvin, E. (2013) Heterogeneous nitrification in a full-scale rapid sand filter treating groundwater. Journal of Environmental Engineering-Asce 139(3), 375-384.

Lytle, D.A., Sorg, T.J., Wang, L.L., Muhlen, C., Rahrig, M. and French, K. (2007) Biological nitrification in a full-scale and pilot-scale iron removal drinking water treatment plant. Journal of Water Supply Research and Technology-Aqua 56(2), 125-136.

Lytle, D.A., White, C., Williams, D., Koch, L. and Nauman, E. (2013) Innovative biological water treatment for the removal of elevated ammonia. Journal American Water Works Association 105(9), 87-88.

Martens-Habbena, W., Berube, P.M., Urakawa, H., de la Torre, J.R. and Stahl, D.A. (2009) Ammonia oxidation kinetics determine niche separation of nitrifying Archaea and Bacteria. Nature 461(7266), 976-979.

Martens-Habbena, W., Berube, P.M., Urakawa, H., de la Torre, J.R., Stahl, D. a, 2009. Ammonia oxidation kinetics determine niche separation of nitrifying Archaea and Bacteria. Nature 461, 976–9.

Martens-Habbena, W. and Stahl, D.A. (2011) Nitrogen metabolism and kinetics of Ammonia-Oxidizing Archaea. Methods in Enzymology 496, 465-487.

451 Martiny, A.C., Albrechtsen, H.J., Arvin, E. and Molin, S. (2005) Identification of bacteria in biofilm and
452 bulk water samples from a nonchlorinated model drinking water distribution system: Detection of a large
453 nitrite-oxidizing population associated with Nitrospira spp. Applied and Environmental Microbiology
454 71(12), 8611-8617.

455 Nitzsche, K.S., Weigold, P., Loesekann-Behrens, T., Kappler, A. and Behrens, S. (2015) Microbial
456 community composition of a household sand filter used for arsenic, iron, and manganese removal from
457 groundwater in Vietnam. Chemosphere 138, 47-59.

458 Niu, J., Kasuga, I., Kurisu, F., Furumai, H. and Shigeeda, T. (2013) Evaluation of autotrophic growth of
459 ammonia-oxidizers associated with granular activated carbon used for drinking water purification by DNA-
460 stable isotope probing. Water Research 47(19), 7053-7065.

461 Palatinszky, M., Herbold, C., Jehmlich, N., Pogoda, M., Han, P., von Bergen, M., Lagkouvardos, I., Karst,
462 S.M., Galushko, A., Koch, H., Berry, D., Daims, H., Wagner, M., 2015. Cyanate as an energy source for
463 nitrifiers. Nature 524, 105–108.

464 Palomo, A., Jane Fowler, S., Gülay, A., Rasmussen, S., Sicheritz-Ponten, T., Smets, B.F., 2016.
465 Metagenomic analysis of rapid gravity sand filter microbial communities suggests novel physiology of
466 Nitrospira spp. ISME J. 10, 2569–2581.

467 Pester, M., Maixner, F., Berry, D., Rattei, T., Koch, H., Lücker, S., Nowka, B., Richter, A., Spieck, E.,
468 Lebedeva, E., Loy, A., Wagner, M., Daims, H., 2014. NxrB encoding the beta subunit of nitrite
469 oxidoreductase as functional and phylogenetic marker for nitrite-oxidizing N itrospira. Environ. Microbiol.
470 16, 3055–3071.

471 Pinto, A.J., Marcus, D.N., Ijaz, Z., Bautista-de los Santos, Q.M., Dick, G.J., Raskin, L., 2015. Metagenomic
472 Evidence for the Presence of Comammox Nitrospira-Like Bacteria in a Drinking Water System. mSphere 1,
473 e00054-15.

Ririe, K.M., Rasmussen, R.P. and Wittwer, C.T. (1997) Product differentiation by analysis of DNA melting curves during the polymerase chain reaction. Analytical Biochemistry 245(2), 154-160.

Rittmann, B.E., Tang, Y., Meyer, K. and Bellamy, W.D. (2012) Water Treatment Plant Design. Association, A.W.W. (ed).

Rotthauwe, J.H., Witzel, K.P. and Liesack, W. (1997) The ammonia monooxygenase structural gene amoA as a functional marker: Molecular fine-scale analysis of natural ammonia-oxidizing populations. Applied and Environmental Microbiology 63(12), 4704-4712.

Sauder, L.A., Peterse, F., Schouten, S., Neufeld, J.D., 2012. Low-ammonia niche of ammonia-oxidizing archaea in rotating biological contactors of a municipal wastewater treatment plant. Environ. Microbiol. 14, 2589–2600.

Sharma, S.K., Petrusevski, B., Schippers, J.C., 2005. Biological iron removal from groundwater : a review. J. Water Supply Res. Technol. 54, 239–247.

Tatari, K., Smets, B.F. and Albrechtsen, H.J. (2016) Depth investigation of rapid sand filters for drinking water production reveals strong stratification in nitrification biokinetic behavior. Water Research.

Valentine, D.L. (2007) Adaptations to energy stress dictate the ecology and evolution of the Archaea. Nature Reviews Microbiology 5(4), 316-323.

van der Wielen, P.W.J.J., Voost, S., van der Kooij, D., 2009. Ammonia-oxidizing bacteria and archaea in groundwater treatment and drinking water distribution systems. Appl. Environ. Microbiol. 75, 4687–95.

van Kessel, M.A.H.J., Speth, D.R., Albertsen, M., Nielsen, P.H., Op den Camp, H.J.M., Kartal, B., Jetten, M.S.M. and Lucker, S. (2015) Complete nitrification by a single microorganism. Nature 528(7583), 555-559.

Verhamme, D.T., Prosser, J.I. and Nicol, G.W. (2011) Ammonia concentration determines differential growth of ammonia-oxidising archaea and bacteria in soil microcosms. Isme Journal 5(6), 1067-1071.

White, C.P., DeBry, R.W. and Lytle, D.A. (2012) Microbial Survey of a Full-Scale, Biologically Active Filter for Treatment of Drinking Water. Applied and Environmental Microbiology 78(17), 6390-6394.

Whitman, W.B., Coleman, D.C. and Wiebe, W.J. (1998) Prokaryotes: The unseen majority. Proceedings of the National Academy of Sciences of the United States of America 95(12), 6578-6583.

Winkler, M.K.H., Bassin, J.P., Kleerebezem, R., Sorokin, D.Y. and van Loosdrecht, M.C.M. (2012) Unravelling the reasons for disproportion in the ratio of AOB and NOB in aerobic granular sludge. Applied Microbiology and Biotechnology 94(6), 1657-1666.

Wuchter, C., Abbas, B., Coolen, M.J.L., Herfort, L., van Bleijswijk, J., Timmers, P., Strous, M., Teira, E., Herndl, G.J., Middelburg, J.J., Schouten, S. and Damste, J.S.S. (2006) Archaeal nitrification in the ocean. Proceedings of the National Academy of Sciences of the United States of America 103(33), 12317-12322.

Zhang, Y., Love, N. and Edwards, M. (2009) Nitrification in drinking water systems. Critical Reviews in Environmental Science and Technology 39(3), 153-208.

509

510 **Table 1.** Selected water quality parameters and characteristics at the 4 investigated DWTPs.

		DWTP 1 (Sjælsø 1)	DWTP 2 (Sjælsø 2)	DWTP 3 (Langerød)	DWTP 4 (Islevbro)
Raw water[i]	NH_4^+ (mg/L)	0.51 ± 0.21	1.08 ± 0.44	1.09 ± 0.17	0.41 ± 0.20
	CH_4 (mg/L)	0.12 ± 0.17	3.73 ± 2.67	0.07 ± 0.04	0.02 ± 0.03
	Fe^{2+} (mg/L)	2.9 ± 1.7	1.9 ± 1.1	3.0 ± 0.2	1.8 ± 1.1
	HCO_3^- (mg /L)	N/A[ii]	N/A	360 ± 8	350 ± 48
	NVOC (mg/L)	2.7 ± 0.4	2.3 ± 0.3	2.6 ± 0.2	2.3 ± 0.3
	Dissolved O_2 (mg/L)	0.65 ± 0.3	0.87 ± 0.4	0.31 ± 0.1	1.1 ± 0.6
	pH	N/A	N/A	7.4 ± 0.1	7.4 ± 0.3
Aeration	Aerator type	Cascade	Intensive tray (INKA)	Cascade	Corrugated plate (Coplator)
Pre-filters	Filter flow (×10^3 L/h)	80	60	100	288
	Active layer depth (m)	0.4 + 0.4	0.3	0.7	2.0
	Material[iii]	1.6-2.5 mm anthracite + 3.0-5.0 mm sand	3.0-5.0 mm sand	2.0-3.0 mm sand	40-50 mm gravel
	Backwashing frequency (d)[iv]	13	10	1	30
	Backwashing procedure	5 m air scouring followed by 5 min water upwash at 1000 m^3/h	3 min air and water flushing followed by 15 min water upwash at 1550 m^3/h	15 min air scouring followed by 4 min water upwash at 920 m^3/h	N/A
After-filters	Filter flow (×10^3 L/h)	52	60	50	72
	Active layer depth (m)	0.4	0.4	0.65	0.7
	Material	1.5-2.0 mm calcined flint	0.8-1.4 mm sand	0.8-1.4 mm sand	0.8-1.2 mm sand
	Backwashing frequency (d)[iii]	12	14	10	14
	Backwashing procedure	5 min air scouring followed by 5 min water upwash at 1000 m^3/h	5 min air scouring followed by 8 min water upwash at 1550 m^3/h	5 min air scouring followed by 5 min water upwash at 600 m3/h	3 min air scouring at 90 m/h followed by water 10 min upwash at 450 m^3/h
Treated water[i]	NH_4^+ (mg/L)	<0.05	<0.05	0.11 ± 0.11	<0.05
	CH_4 (mg/L)	N/A	N/A	<0.01	<0.01
	Fe^{2+} (mg/L)	<0.1	<0.1	<0.1	<0.1
	HCO_3^- (mg /L)	N/A	N/A	360 ± 8	350 ± 13
	NVOC (mg/L)	2.4 ± 0.5	3.3± 0.6	2.5 ± 0.3	2.2 ± 0.1
	Dissolved O_2 (mg/L)	N/A	N/A	9.7 ± 0.5	8.7 ± 0.4
	pH	N/A	N/A	7.7 ± 0.1	7.4 ± 0.1

511 i. Water quality data are means provided by the DWTPs
512 ii. N/A: Not Available
513 iii. Nominal size range before filter start-up. Actual filter material size may be different due to mineral deposition on the filter material
514 iv. Backwashing frequency is regulated from the total filter flow. Calculation of average backwashing interval here is based on the
515 average filter flow

516 **Table 2.** Filter material bulk densities and microbial densities per mass and per volume of filter material.
517 Reported values are means calculated from equal weighing of measured values at all depths, sampling
518 locations in a filter and parallel filters at each DWTP. Mean values are reported with their standard deviation.

519

	Filter material bulk density					
	Pre-filters			After-filters		
	(×10^6 g/m^3 filter material)		N[i]	(×10^6 g/m^3 filter material)		N[i]
DWTP 1	1.0 ± 0.25		6	1.2 ± 0.06		12
DWTP 2	1.4 ± 0.04		5	1.5 ± 0.03		11
DWTP 3-E	1.7 ± 0.05		6	1.6 ± 0.05		13
DWTP 3-W	1.5 ± 0.07		5	1.6 ± 0.05		14
DWTP 4	N/S		-	1.5 ± 0.28		12
	Total bacteria (*Eubacteria*)[iii]					
	Mass density	Volumetric density[ii]	N	Mass density	Volumetric density	N
	(×10^9 copies/g)	(×10^{15} copies/m^3)		(×10^9 copies/g)	(×10^{15} copies/m^3)	
DWTP 1	2.0 ±1.0	1.8 ± 0.56	6	0.9 ± 2.2	1.1 ± 0.27	29
DWTP 2	12 ± 4.6	16 ± 6.1	14	1.6 ± 6.3	2.5 ± 0.97	30
DWTP 3-E	3.1 ±1.2	5.1 ± 2.0	11	3.5 ± 17	5.7 ± 2.9	26
DWTP 3-W	6.6 ±1.7	9.8 ± 2.7	5	4.0 ±17	6.5 ±2.8	32
DWTP 4	N/S[v]	N/S	-	8.8 ±13	11 ±16	40
	AOB (*Nitrosomonas* spp and *Nitrosospira* spp)[iii]					
	(×10^7 copies/g)	(×10^{13} copies/m^3)		(×10^7 copies/g)	(×10^{13} copies/m^3)	
DWTP 1	19 ± 16	16 ± 12	11	0.41 ± 17	0.49 ± 0.21	30
DWTP 2	13 ± 6.5	17 ± 8.7	14	2.0 ± 0.88	3.0 ± 1.4	30
DWTP 3-E	5.8 ± 4.2	9.6 ± 6.8	11	15 ± 14	24 ± 22	26
DWTP 3-W	23 ± 7.8	35 ± 12	5	12 ± 12	20 ± 19	25
DWTP 4	N/S	N/S	-	1.2 ± 2.3	1.3 ± 2.5	35
	***Nitrobacter*[iii]**					
	(×10^4 copies/g)	(×10^{10} copies/m^3)		(×10^4 copies/g)	(×10^{10} copies/m^3)	
DWTP 1	7.8 ± 1.5	7.6 ± 2.0	12	3.0 ± 1.8	3.6 ± 2.1	12
DWTP 2	370 ± 230	500 ± 310	14	19 ± 7.9	29 ± 12	10
DWTP 3-E	8.7 ± 3.0	15 ± 4.9	17	6.1 ± 0.91	10 ± 15	7
DWTP 3-W	23 ± 16	34 ± 23	10	5.4 ± 4.0	8.6 ± 6.3	11
DWTP 4	N/S	N/S	-	9.7 ± 16	11 ± 16	36
	***Nitrospira*[iii]**					
	(×10^8 copies/g)	(×10^{14} copies/m^3)		(×10^8 copies/g)	(×10^{14} copies/m^3)	
DWTP 1	3.4 ± 2.3	3.8 ± 3.4	17	0.81 ± 0.21	0.97 ± 0.26	17
DWTP 2	24 ± 13	33 ± 17	15	3.3 ± 1.1	5.1 ± 1.7	25
DWTP 3-E	1.7 ± 0.88	2.8 ± 1.4	10	5.2 ±4.1	8.6 ± 6.9	23
DWTP 3-W	5.9 ± 0.85	8.8 ± 1.4	5	8.9 ± 5.4	14 ±8.8	23
DWTP 4	N/S	N/S	-	8.4 ± 13	9.7 ± 14	46
	AOA[iv]					
	(×10^3 copies/g)	(×10^9 copies/m^3)		(×10^3 copies/g)	(×10^9 copies/m^3)	
DWTP 1	6.0 ± 3.9	5.7 ± 3.3	12	18 ± 14	21 ± 17	18
DWTP 2	15 ± 11	20 ± 15	14	3.8 ± 1.7	5.7 ± 2.6	15
DWTP 3-E	2.3 ± 1.1	3.9 ± 1.9	17	< 1[vi]	< 1.6[vi]	-
DWTP 3-W	2.6 ± 2.5	4.0 ± 3.8	5	< 1[vi]	< 1.6[vi]	-
DWTP 4	N/S	N/S	-	320 ± 120	460 ± 260	6

i. Number of samples used to calculate mean density values
ii. Conversion from filter material mass to volume units was done by multiplying with the mean bulk density
iii. Quantified by 16S rRNA targeted qPCR, iv. Quantified by *amo*A targeted qPCR
v. N/S: Not sampled due to coarse filter material in the pre-filter at DWTP 4
vi. Densities below detection limit

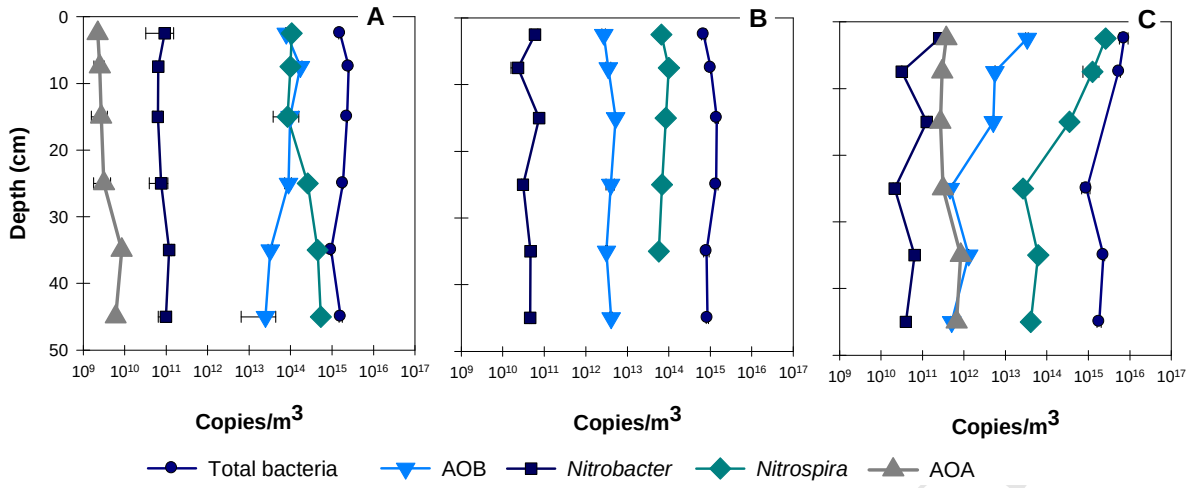

521

522 **Figure 1.** Depth profiles of the volumetric densities at one location of: one pre-filter at DWTP 1 (Panel A),
523 one after-filter at DWTP 1 (Panel B) and one after-filter at DWTP 4 (Panel C). Densities were quantified by
524 qPCR and error bars represent the standard deviation of the analytical method.

525

526

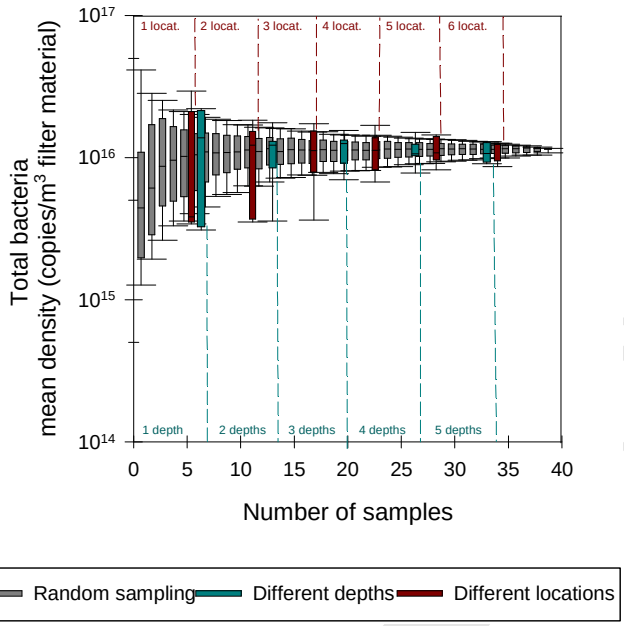

527

528 **Figure 2.** Distribution of total bacterial mean density at DWTP 4 based on sample number and sampling
529 strategy. Random sampling includes all random combinations of samples at different depths, locations and
530 parallel after-filters. Sampling at different depths includes all locations at these specific depths and sampling
531 at different locations includes all depths at these specific locations.

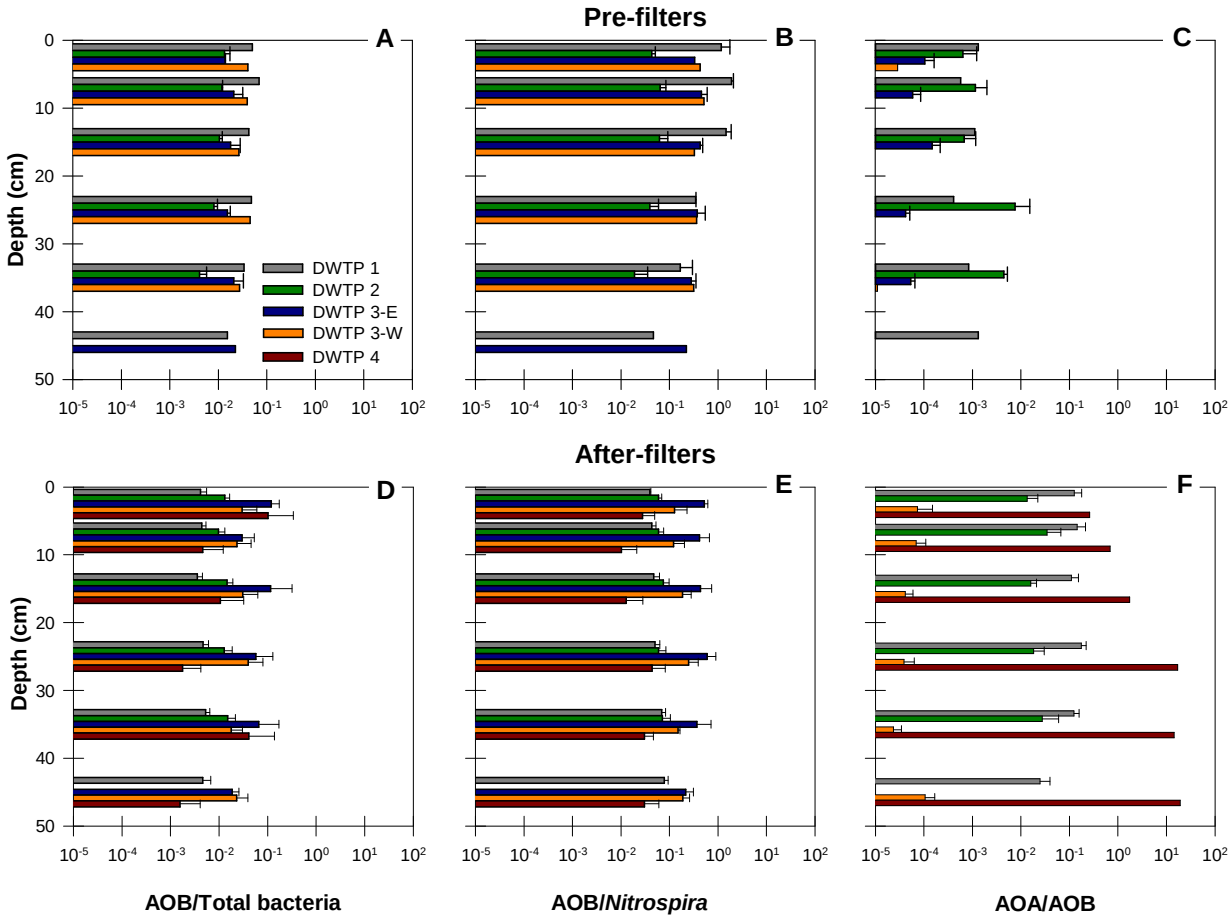

532

533 **Figure 3.** Density ratios in the pre-filters (Panels A-C) and after-filters (Panels D-F) at all investigated
534 DWTPs. Panels A and D: ratio of AOB to total bacteria quantified by 16S rRNA-specific qPCR; Panels B
535 and E: ratio of AOB to *Nitrospira* quantified by 16S rRNA-specific qPCR; Panels C and F: ratio of AOA to
536 AOB quantified by the *amo*A-specific qPCR. Bars are means of all the sampled locations in all parallel
537 filters and error bars are the standard deviation of the mean.

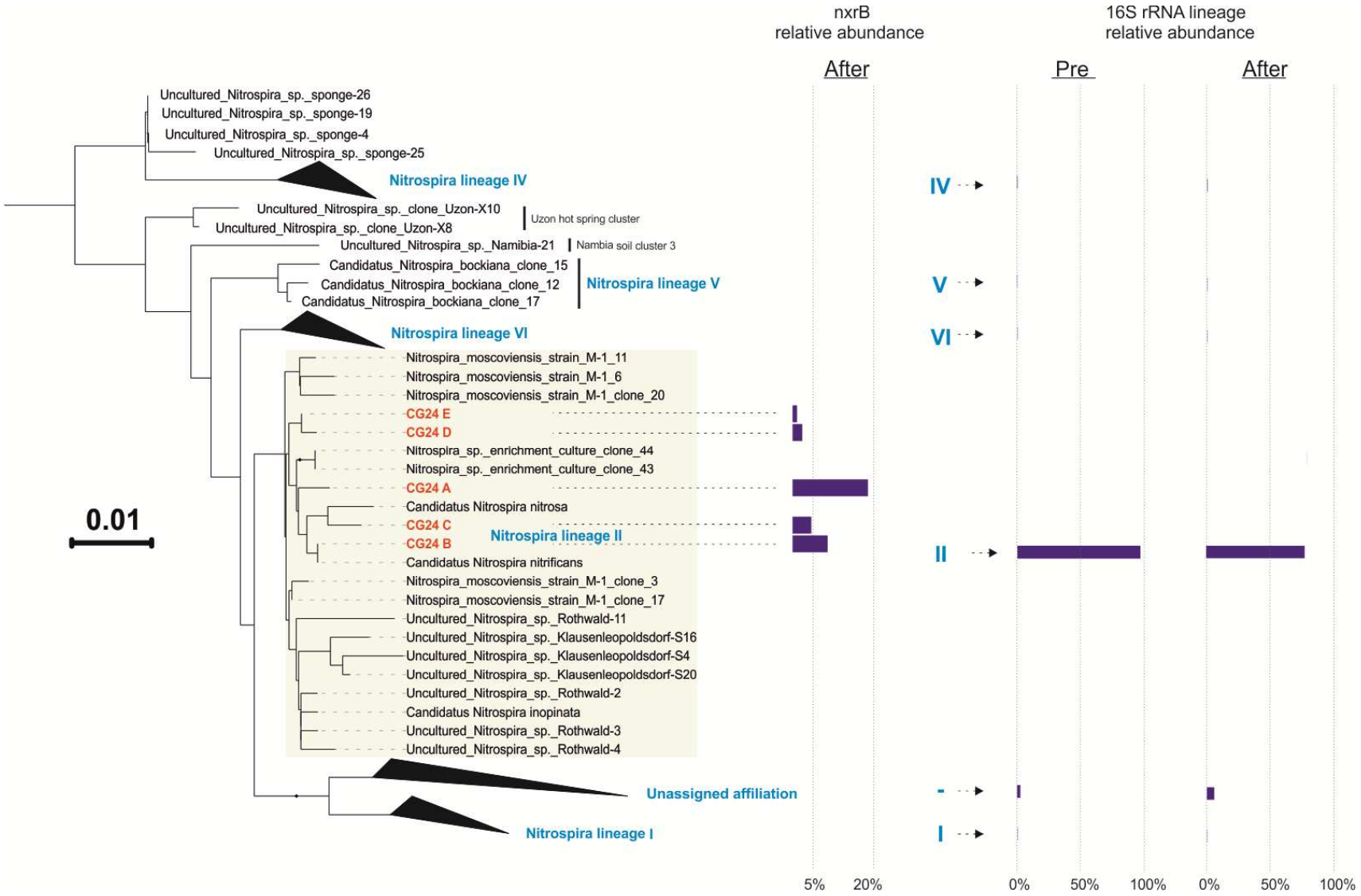
nxrB
relative abundance
16S rRNA lineage
relative abundance
After
Pre
After
Uncultured_Nitrospira_sp._sponge-26
Uncultured_Nitrospira_sp._sponge-19
Uncultured_Nitrospira_sp._sponge-4
Uncultured_Nitrospira_sp._sponge-25
Nitrospira lineage IV
Uncultured_Nitrospira_sp._clone_Uzon-X10
Uncultured_Nitrospira_sp._clone_Uzon-X8
Uzon hot spring cluster
Uncultured_Nitrospira_sp._Namibia-21
Nambia soil cluster 3
Candidatus_Nitrospira_bockiana_clone_15
Candidatus_Nitrospira_bockiana_clone_12
Candidatus_Nitrospira_bockiana_clone_17
Nitrospira lineage V
Nitrospira lineage VI
Nitrospira_moscoviensis_strain_M-1_11
Nitrospira_moscoviensis_strain_M-1_6
Nitrospira_moscoviensis_strain_M-1_clone_20
CG24 E
CG24 D
Nitrospira_sp._enrichment_culture_clone_44
Nitrospira_sp._enrichment_culture_clone_43
CG24 A
Candidatus Nitrospira nitrosa
CG24 C
CG24 B
Nitrospira lineage II
Candidatus Nitrospira nitrificans
Nitrospira_moscoviensis_strain_M-1_clone_3
Nitrospira_moscoviensis_strain_M-1_clone_17
Uncultured_Nitrospira_sp._Rothwald-11
Uncultured_Nitrospira_sp._Klausenleopoldsdorf-S16
Uncultured_Nitrospira_sp._Klausenleopoldsdorf-S4
Uncultured_Nitrospira_sp._Klausenleopoldsdorf-S20
Uncultured_Nitrospira_sp._Rothwald-2
Candidatus Nitrospira inopinata
Uncultured_Nitrospira_sp._Rothwald-3
Uncultured_Nitrospira_sp._Rothwald-4
Unassigned affiliation
Nitrospira lineage I
0.01
IV
V
VI
II
-
I
5%
20%
0%
50%
100%
0%
50%
100%

538

539 **Figure 4.** Phylogenetic analysis of *nxrB* genes retrieved from the CG24 *Nitrospira* population genome
540 (Palomo et al., 2016) with NCBI database recorded sequences as reference (Pester et al., 2014). The scale bar
541 indicates 1% estimated sequence divergence. Relative abundance of CG24 *nxrB* genes (compared to total
542 *nxrB* gene in the community metagenome) and relative abundance of *Nitrospira* 16S rRNA sublineages
543 (compared to all *Nitrospira* sequences) sequences are reported.

544

545

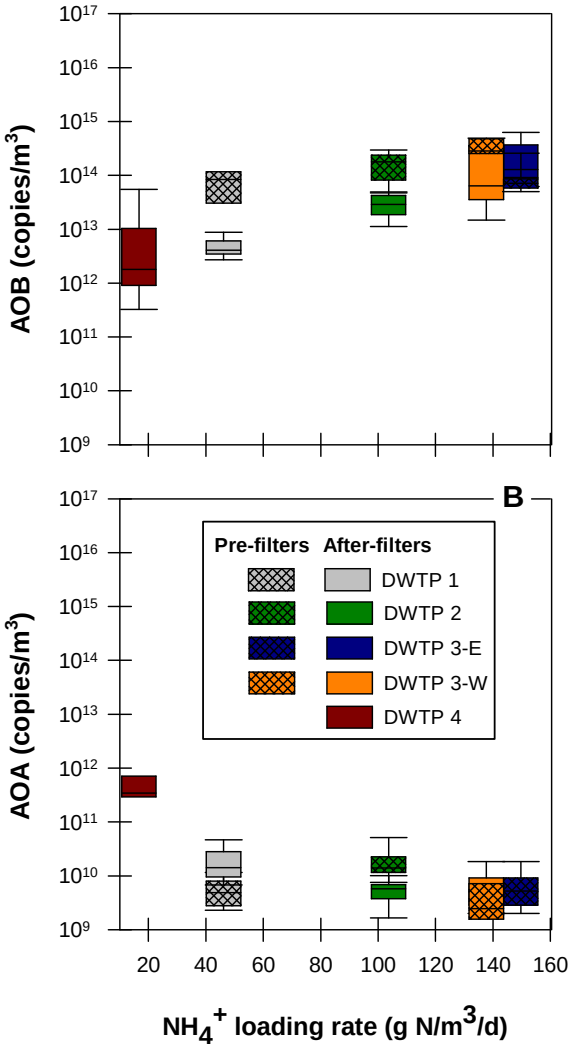

546

547 **Figure 5.** Volumetric densities of AOB (Panel A) and AOA (Panel B) in the investigated pre- and after-
548 filters as a function of the NH_4^+ loading rate to the DWTP.

549

Highlights

- Microbial density in RSFs are high (upto10^9 to 10^{10} per gram (10^{15} to 10^{16} per m^3) but vary spatially.
- Acceptable mean precision of density estimates requires 7 random samples.
- *Nitrospira* were more abundant than *Nitrobacter* and AOBs.
- Nitrospira abundance is likely caused by their NH_4^+ oxidation capability (comammox).
- AOB consistently exceed AOAs in RSFs, except in RSFs with strong stratification.